Journal of Aerospace Technology and Management
ISSN: 1984-9648
secretary@jatm.com.br
Instituto de Aeronáutica e Espaço
Brasil

Schuch, Daniel; Fisch, Gilberto
The Use of an Atmospheric Model to Simulate the Rocket Exhaust Effluents Transport and Dispersion for the Centro de Lançamento de Alcântara
Journal of Aerospace Technology and Management, vol. 9, núm. 2, abril-junio, 2017, pp. 128-137
Instituto de Aeronáutica e Espaço
São Paulo, Brasil

doi: 10.5028/jatm.v9i2.740

The Use of an Atmospheric Model to Simulate the Rocket Exhaust Effluents Transport and Dispersion for the Centro de Lançamento de Alcântara

Daniel Schuch[1], Gilberto Fisch[2]

ABSTRACT: This paper introduces a new approach to represent the rocket exhaust effluents into an atmospheric dispersion model considering the trajectory and variable burning rates of a Satellite Vehicle Launcher, taking into account the buoyancy of the exhausted gases. It presents a simulation for a Satellite Vehicle Launcher flight at 12:00Z in a typical day of the dry season (Sept 17, 2008) at the Centro de Lançamento de Alcântara using the Weather Research and Forecasting Model coupled with a modified chemistry module to take into account the gases HCl, CO, CO_2, and particulate matter emitted from the rocket engine. The results show that the HCl levels are dangerous in the first hour after the launching into the Launch Preparation Area and at the Technical Meteorological Center region; the CO levels are critical for the first 10 min after the launching, representing a high risk for human activities at the proximities of the launching pad.

KEYWORDS: Satellite Vehicle Launcher, Mesoscale model, Atmospheric dispersion model, HCl.

INTRODUCTION

The Centro de Lançamento de Alcântara (CLA) is the Brazilian access to the space, located at the north part of the northeastern region of Brazil. It has some advantages due to its geographical position close to the Equator, which allows rocket launchings that consume less propellant for geostationary satellite missions. Other advantages are associated with its proximity of São Luís (capital of Maranhão State) as well as its low population density, so the health risks of contamination by gases sent out from launchings are reduced. Rockets such as the Veículo Lançador de Satélites (VLS) are launched from this Range Center.

During the first few seconds following the ignition of the engine, the VLS releases a large cloud of hot, buoyant exhaust products near the ground level which rise and entrain into atmosphere until reach an approximate equilibrium with the ambient conditions. This cloud is composed by the products of the combustion of perchlorate and aluminum: hydrogen chloride (HCl), water (H_2O), carbon monoxide (CO), carbon dioxide (CO_2), and particulate material composed by aluminum oxide (Al_2O_3) used into the grain composition of the solid propellant (Denison *et al.* 1994).

All the Space Centers around the world have adopted some models in order to predict these gases dispersions. For instance, the East US Space Ranger Center (like NASA JFK/U. S. Cape Canaveral) uses an operational model known as Rocket Exhaust Effluent Diffusion Model (REEDM) and it has been used to assess the environmental impact of aerospace activities (Bjorklund

1.Departamento de Ciência e Tecnologia Aeroespacial – Instituto Tecnológico de Aeronáutica – Programa de Pós-Graduação em Ciências e Tecnologias Espaciais – São José dos Campos/SP – Brazil. **2.**Departamento de Ciência e Tecnologia Aeroespacial – Instituto de Aeronáutica e Espaço – Divisão de Ciências Atmosféricas – São José dos Campos/SP – Brazil.

Author for correspondence: Daniel Schuch | Departamento de Ciência e Tecnologia Aeroespacial – Instituto Tecnológico de Aeronáutica – Programa de Pós-Graduação em Ciências e Tecnologias Espaciais | Praça Marechal Eduardo Gomes, 50 – Vila das Acácias | CEP: 12.228-901 – São José dos Campos/SP – Brazil | Email: underschuch@gmail.com

Received: Jul. 19, 2016 | **Accepted:**Oct. 12, 2016

et al. 1982). This dispersion model is based on Gaussian model concepts: the exhaust material (mixture amongst CO, CO_2, HCl, and Al_2O_3) is assumed to be uniformly and vertically distributed and to have a bivariate Gaussian distribution in the plane of the horizon at the point of cloud stabilization, which is determined by the cloud rise theory.

The model used at the European Spaceport of Kourou (French Guyana) is the SARRIM Software (Cencetti *et al*. 2011), which considers the emissions divided into "puffs" from the launching pad up to the stabilization height, dealing with the local and large scale impact assessment for propellant and hypergolic rocket releases. It is an operational and fast running tool taking into account atmospheric thermal stratifications inside the boundary layer using *in situ* data like radiosondes.

The India Space Center (Satish Dhawan Space Center SDCS SHAR) has coupled a Hybrid Single-Particle Lagrangian Integrated Trajectory (HYSPLIT) model with an atmospheric mesoscale one (in this case, it was used the mesoscale meteorological model-MM5) to predict the dispersion of exhaust pollutant in the form of vapor and ground level concentrations (Rajasekhar *et al.* 2011).

The Brazilian community is also addressing this problem for CLA since 2010 and it was developed the Modelo Simulador da Dispersão de Efluentes de Foguetes (MSDEF), which represents the solution for time-dependent advection-diffusion equation applying the Laplace transform considering the Atmospheric Boundary Layer as a multilayer system. This solution allows a time evolution description of the concentration field emitted from a source during a release lasting time; it takes into account deposition velocity, first-order chemical reaction (decay), gravitational settling, precipitation scavenging, and plume rise effect. A detail description of this model can be found in Moreira *et al*. (2011). In Nascimento *et al.* (2014), the authors coupled this model to the Weather Research and Forecasting Model (WRF), for the meteorological forecast, and to the Community Multi-scale Air Quality model (CMAQ), for the chemistry. Moreover, Iriart and Fisch (2016) used the WRF coupled with this chemistry module (Chem). Both studies addressed the CLA dispersion problem for air quality models.

In this study we propose a new representation of a rocket emission, taking into account the plume rise effect, trajectory, and variable emissions rates (in time and space), into a meteorological/chemical model in order to achieve a better vertical distribution of the emissions and then predict the transport, dispersion, and atmospheric reaction of the gas exhausted. A simulation using data of the Brazilian VLS was assessed using the WRF model (version 3.7.1) with a modified Regional Atmospheric Chemistry Mechanism (which includes HCl) for the CLA region.

METHODOLOGY

The WRF model is a numerical weather prediction system, considered the state-of-the-art, designed for both atmospheric research and operational forecasting needs, being applied to a wide range of meteorological problems with scales from tens of meters to thousands of kilometers. The coupling of the meteorology and chemistry (into the WRF-Chem coupled) is calculated on-line (without loss of information), and the meteorological process of transport, radiation, and reactions is fully coupled (interacting with each other) and solved simultaneously without any type of interpolation (Grell *et al*. 2005; Skamarock *et al*. 2008).

For the simulations, 3 nested domains centered into the Setor de Preparação de Lançamento (SPL), where the rocket is launched, were chosen. The outer domain (d1) is a 100 × 100 grid points with 9 km of horizontal resolution; the middle domain (d2) has 70 × 70 points and 3 km of resolution; the inner domain (d3) has 40 × 40 points with 1 km of horizontal resolution. All domains have 43 vertical levels, from surface up to 30 km, distributed mainly close to the surface. Figure 1a shows an image of the region and the 3 domains.

The static data (topography, land mask, vegetation, etc.) used was provided by the United States Geological Survey (available from: http://www.mmm.ucar.edu/wrf/src/WPS_files/geog.tar.gz) with spatial resolution of 30" (this data is usually used to weather forecasts). Figure 1b shows the topography (lines) and landmask (colors) for the inner domain (d3). Also, it was marked the position of some buildings that are part of the CLA's structure: SPL and the Setor de Meteorologia (SMT), as well as the only habited areas nearby: the city of Alcântara (CLA) and the Tapireí village (VTA).

The meteorological variables data were extracted from analysis of the Global Forecasting System (GFS) with spatial resolution of 0.5° and available every 3 h. This option was chosen as this meteorological inputs are operational from the National Centers for Environmental Prediction (NCEP). The chemical species used was obtained from the Model for Ozone and Related chemical Tracers-4 (Emmons *et al*. 2010), and the initial and boundary states were modified with the MOZBC pre-processor (Pfister *et al*. 2011).

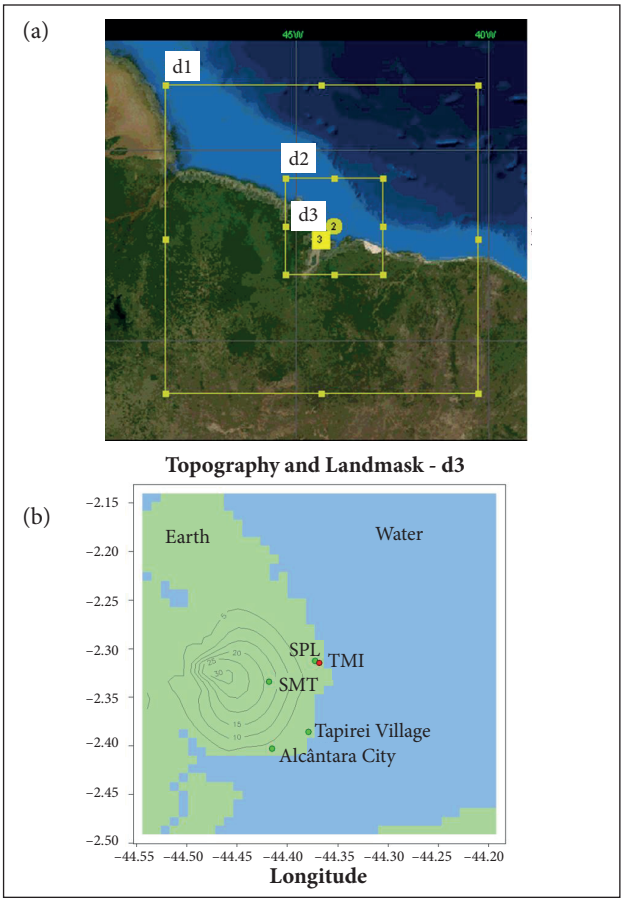

Figure 1. (a) Domains of simulation; (b) Topography (lines) and landmask (green for continent and blue for water) of inner domain.

For the WRF configuration, it was used the following set of parametrizations:

- Microphysics: WRF Single-Moment 3-class Scheme, simple and efficient scheme which contains ice process adapted to large scale.
- Long wave radiation: Rapid Radiative Transfer Model (RRTM), a scheme which utilizes tables of radiation efficiency.
- Short wave radiation: Dudhia scheme, simple scheme of integration which allows the absorption of radiation in clear sky from the clouds and scattering by atmosphere.
- Superficial layer: MYNN surface layer, Nakanishi and Niimo scheme.
- Surface: Noah Land Surface Model, scheme of soil temperature and humidity with 4 layers.
- Planetary Boundary Layer (PBL): Mellor Yamada Nakanishi and Nimo level 2.5, scheme with prediction of turbulent kinetic energy to the model sub-grid.
- Cumulus: Grell 3D, enhanced scheme of Grell-Devenyi which can be used for high spatial resolutions (turned off in the d3 domain).

Due to the necessity of representing all the emitted species by the combustion of the rocket solid propellant into the WRF model, especially the species HCl, a new chemistry mechanism based on the RACM (Stockwell *et al.* 1997) was created. HCl and more 5 chlorinated species were added (Cl, Cl_2, HOCl, ClO, and formyl fluoride), as well as 3 photoreactions, 5 inorganic reactions, and 11 organic reactions from the CB05 mechanism (Yarwood *et al.* 2005) inside the RACM.

Since version 2.2, the WRF model was released with the kinetic preprocessor (KPP) built in the source code. It was designed as a general analysis tool to facilitate the numerical solution of chemical reaction network problems. The KPP subroutines automatically generate FORTRAN code that computes the time-evolution of chemical species, starting with a specification of the chemical mechanism. KPP further allows a rich selection of numerical integration schemes and provides a framework for evaluation of new integrators and chemical mechanisms (Damian *et al.* 2002).

The interaction of the KPP and WRF is made by a subprogram named WRF-KPP-Coupler (WKC). Once the KPP option is enabled, the WRF's compilation script compiles and executes the WKC, and the KPP generates all the code to compile WRF, including the new mechanism. Even though the WKC generates the code to be integrated into the model, the mechanism needs to be included to the file Registry.chem in order to be recognized by the model. Consequently, the Chem module must be modified in order to include the new mechanism in the processes of initialization, calculation of velocities of deposition, different emission options, and optical proprieties.

REPRESENTATION OF SATELLITE VEHICLE LAUNCHER EMISSIONS

In air quality (AQ) models, the way emissions are represented is the most critical input parameter and has greater impact into the final concentration of the contaminant. The inclusion of a source like the VLS into WRF needs some considerations: the rocket like the fuel expenditure, vertical trajectory, and the type of propellant used should be taken into account as well as the limitations of the model for time and space scales.

The total mass of gases released into atmosphere in a VLS launch is given by:

$$M = \int_{t_0}^{t_N} \frac{\partial M}{\partial t} dt \quad (1)$$

where: $\partial M/\partial t$ is the fuel expenditure rate (g/s), which varies with time along the trajectory of the rocket; t_0 is the ignite time; and t_N is the time when the fuel is completely burned.

As the shortest interval for data input of WRF is 1 min, the emissions were split in min by min as

$$M = M_1 + M_2 + \ldots + M_n + \ldots + M_N = \quad (2)$$
$$= \int_{t_0}^{t_1} \frac{\partial M}{\partial t} dt + \int_{t_1}^{t_2} \frac{\partial M}{\partial t} dt + \ldots + \int_{t_{n-1}}^{t_n} \frac{\partial M}{\partial t} dt + \ldots + \int_{t_{N-1}}^{t_N} \frac{\partial M}{\partial t} dt$$

where: $t_n = 60n$ (s), and each term represents an emission file for the model.

For the vertical domain, the WRF model was discretized into sigma levels, which is a normalized coordinate (assuming unitary value at surface and 0 on the top of the domain) following the topography (Fig. 2).

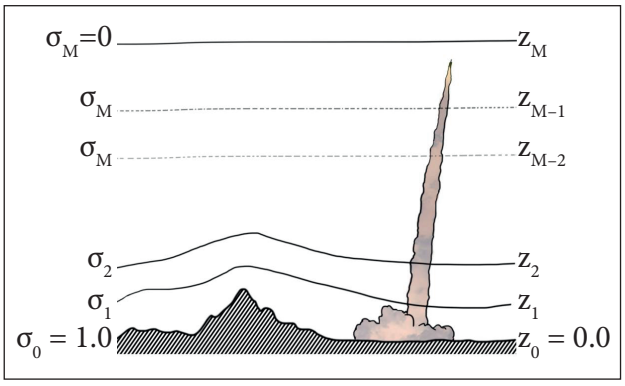

Figure 2. Layers and the rocket trajectory.

Whereas the rocket it is not a fixed source, the distribution of emission should follow the rocket trajectory and is allocated into M model layers as follows:

$$M_n = \sum_{m=1}^{M} M_{nm} = M_{n1} + M_{n2} + \ldots + M_{nm} + \ldots + M_{nM} \quad (3)$$

where:

$$M_{nm} = \int_{t_{n-1}}^{t_n} H\left((z_{m-1} - z)(z_m - z)\right) \frac{\partial M(t,z)}{\partial t} dt \quad (4)$$

H is the Heaviside function (whose value is 0 for negative and 1 for positive argument); z_m is the height of the top of the layer m; z_{m-1} is the top of the layer below the surface (z_0); $\partial M/\partial t$ is function of height and time.

For VLS emission scenarios, the exhaust from the rocket combustion is at several thousand Kelvin degrees and highly buoyant. The high temperature of these exhaust emissions causes the plume to be less dense than the surrounding atmosphere, and buoyancy forces acting on the cloud can cause it to lift off the ground and accelerate vertically. As the buoyant cloud rises, it entrains ambient air and grows in size while also cooling. In this initial cloud rise phase, the growth of the cloud volume is due primarily to internal velocity gradients and mixing induced by large temperature gradients within the cloud itself. Even though the cloud is entraining air and cooling due to the mixing hot combustion gases with cooler ambient air, the net thermal buoyancy in the cloud is conserved, and the cloud will continue to rise until it either reaches a stable layer in the atmosphere or the cloud vertical velocity becomes slow enough to be damped by viscous forces (Nyman 2009).

Considering that the WRF model does not have a general scheme for plume rise, we have assumed that the plume is released into a height matching the rocket trajectory plus a plume rise (Δz) height. For the determination of this height rise, the following parametrizations were adopted, in which the height is calculated directly by a model based on Briggs (1975).

For an instantaneous cloud rise scheme, this rise is defined as

$$\Delta z_i = \left(\frac{8F_i}{\gamma^3 s}\right)^{1/4} \quad (5)$$

where: F_i = buoyancy term = $3gq/4\pi\rho C_\rho T_a$; T_a(m^{4}s^2) is the ambient temperature (K); ρ is the air density (kg/m^3); C_p is the specific heat of exhaust cloud gases = 1.7755 (cal/kgK); q = initial heat of the plume = H ($\partial M/\partial t$) δt (cal); H is the effective fuel heat content (cal/g); γ is the air entrainment coefficient = 0.64 (dimensionless); s = atmosferic stability parameter $g/\theta_0(\Delta\theta_0/\Delta z)$(s^{-1}); g is the gravitational acceleration constant = 9.81 (m/s^2); θ_0 = potencial temperature of ambient air = $T_a(p_0/p)^{R/C_p}$ (K).

The time for the ground cloud reaches a height z_k in a stable atmosphere given by

$$t_i = s^{-1/2} \cos^{-1}\left(1 - \left(\frac{s\gamma^3 z_k^4}{4F_i}\right)\right) \quad (6)$$

where: t_i is constrained to be less than the cloud stabilization time:

$$t^* = \frac{\pi}{\sqrt{s}} \tag{7}$$

The height of the rise in a continuous plume in a stable atmosphere is defined as

$$\Delta z_c = \left(\frac{6F_c}{u\gamma^2\sqrt{s}} \right)^{1/3} \tag{8}$$

where: F_c = buoyancy term = $gq/\pi\rho C_p T_a$ (m^4s^2) ; γ is the air entrainment coefficient = 0.5 (dimensionless).

And the time for a continuous plume to reach the height z_k in a stable atmosphere is given by

$$t_c = s^{-1/2} \cos^{-1}\left(1 - \left(\frac{su\gamma^2 z_k^3}{3F_c}\right)\right) \tag{9}$$

where: t_c is constrained to be less than t^*, described by Eq. 7, and u is the wind velocity (Bjorklund *et al.* 1982).

The following equation was based on a solution of the Newton's second law and solved iteratively to predict the motion of a buoyant cloud in the atmosphere, resulting in cloud stabilization height:

$$\Delta z_n(t) = \left[\frac{3F_m}{u\gamma^2\sqrt{s}} \sin(t\sqrt{s}) + \frac{3F_c}{u\gamma^2\sqrt{s}} \left(1 - \cos(t\sqrt{s})\right) + \left(\frac{r_0}{\gamma}\right)^3 \right]^{1/3} - \frac{r_0}{\gamma} \tag{10}$$

where: F_m is the initial vertical momentum = $r_0 w_0 u$ (m^4s^2); r_0 is the initial plume cross-sectional radius = 3.5 (m); w_0 is the initial vertical velocity (m/s); u is the mean ambient wind speed (m/s); γ is the air entrainment coefficient = 0.33 (dimensionless); ρ is the density of exhaust gases = 0.109 (kg/m^3).

A critical parameter in the cloud rise equation is the rate of ambient air entrainment that is defined by γ. Cloud growth as a function of altitude is assumed to be linearly proportional, and the air entrainment coefficient have been compared from the literature (observations and measurements of Titan IV rocket ground clouds), and an empirical cloud rise air entrainment coefficient has been derived from the test data (Nyman 2009). It should be noticed that there is no data of this nature for VLS.

Considering the different formulations from Eqs. 5 to 10, Briggs (1975) suggests that the value of the rise height increment to be used is the smallest between Δz_i, Δz_c, and Δz_n. This suggestion is the most prudent due to the fact that, as the rise effect is larger, the concentration values obtained at surface level are smaller, reducing the risk of underestimating the value of these concentrations.

Once the plume rise height is calculated, the emission into the WRF model can be written as

$$E_n(i,j,m) = \int_{t_{n-1}}^{t_n} H\left((z_{m-1} - z)(z_m - z)\right) \frac{\partial M(t, z + \Delta z(t^*))}{\partial t} dt \tag{11}$$

when $i = i_{TMI}$ and $j = j_{TMI}$ or

$$E_n(i,j,m) = 0 \tag{12}$$

where: $i \neq i_{TMI}$ or $j \neq i_{TMI}$. The indexes i and j are horizontal grid coordinates of the model.

The rocket is launched from the point (i_{TMI}, j_{TMI}) of the WRF inner domain of simulation (d3). Note that Eqs. 11 and 12 disregard the horizontal component of the rocket displacement, but it is a fine assumption even into the finest scale models.

Table 1 shows the composition of the exhaust gases of the VLS, the mass percentage gas, and the variable into WRF. HCl, CO, and CO_2 are pollutants into gaseous form, and Al_2O_3 is divided into 2 sizes of particulate matter of 2.5 mm (pm 2.5) and 10 mm (pm 10).

Table 1. Composition of the exhaust gases of VLS.

Species		%	Variable
Alumina	Al_2O_3	28.4	pm 2.5 + pm 10
Carbon monoxide	CO	28.7	CO
Hydrogen chloride	HCl	21.4	HCl
Nitrogen	N_2	8.3	-
Water vapor	H_2O	6.8	-
Carbon dioxide	CO_2	3.6	CO_2
Hydrogen	H_2	2.8	-

The emissions were generated with a pre-processor named ANTHRO_EMISS, and these files were edited into R software, a language for statistical computing (R Core Team 2015). All emissions were set to 0, and just the rocket emissions are presented in the simulations at the time of launching, which was 12:00Z, using the meteorological output from WRF, the VLS data, and the equations described above.

RESULTS AND DISCUSSION

For the simulations, we have chosen a typical clear sky day from the dry season (Sept 17, 2008), where the model started at 00:00Z and the release of VLS gases occurred at 12:00Z, considering 12 h for the model spin-up. With a radiosonde released at 11:32Z, the mean wind within the planetary boundary layer (about 600 m) is about 13 m/s and the atmospheric stability is unstable, favoring the turbulence. These are characteristics of a suitable day for a rocket launching (wind speed below 10 m/s at surface level, lower wind speed up to 5 km, no rain, etc.) and good conditions for dispersion (presence of an atmosphere unstable) and transport (strong influences of the trade winds) of the rocket effluents.

Figure 3 shows the vertical distribution of the VLS emissions using Eq. 12 for the VLS data and the distribution used by Nascimento *et al.* (2014) for a hypothetical launching of a Titan-IV rocket. It can be observed that the distribution of emissions for the VLS is quite different from Titan-IV: it is lower close to the surface and higher at 1 – 2 km.

Figure 4 shows a time sequence of arrow plots of the horizontal component of the wind at the surface level, whose direction is predominantly from east. The wind speed is above 7 m/s in the ocean region and becomes weaker inland the continent (about 6 m/s in the SPL). The shaded areas represent the HCl concentration at the first layer of the model (approximately 40 m) for the initial 30 min after the launching of VLS. These plots have a log scale for the concentration for a better visualization. In this figure we can observe the exhausted cloud behaviors after the rocket launching: initially it presents a maximum concentration at the launch pad (SPL and TMI) and it is advected and dispersed with time. This plume reached the SMT with a still higher concentration (around 176 ppmv) within about 10 min. The other locations (CLA and VTA) were not reached by this plume. HCl is a colorless gas with an irritating pungent odor perceivable at 0.8 ppmv (Lide 2003). Table 2 presents the hydrogen chloride exposure limits (Braxter *et al.* 2000).

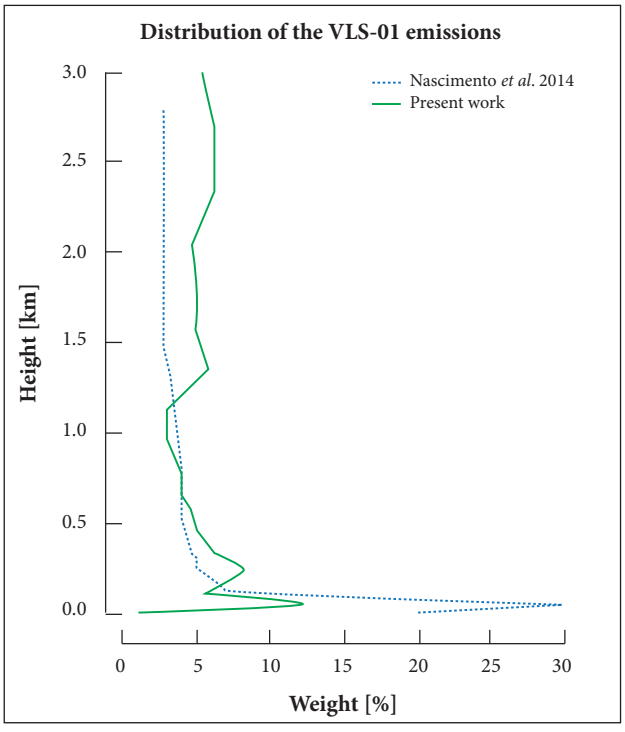

Figure 3. Emissions for the VLS and Titan-IV.

Table 2. Health effects of respiratory exposure to HCl concentration.

HCl exposure limits (ppmv)	Health effects
5 <	Coughing
35	Throat irritation occurs after only a short time
35 <	Severe breathing difficulties and skin inflammation or burns
10 – 50	Maximum level that can be sustained for several hours
100 <	Swelling of the lungs and often throat spasm
50 – 1,000	Maximum possible exposure: 1 h
1,000 – 2,000	Very dangerous even for a very short exposure

Source: extracted from Braxter *et al.* (2000).

Figure 4b presents the same information of Fig. 4a for CO concentrations and it is different from Iriart and Fisch (2016) by 2 reasons: the amount of gases exhausted is associated with a real value for VLS launching and this material is released during the flights trajectory (vertical dependence). For this variable we can notice the larger areas with higher concentrations that persist beyond the plume passage. However, this variable is not so toxic as HCl.The CO is a colorless and odorless gas that is slightly less dense than air. It is toxic to humans (and another hemoglobic animals) when observed in concentrations above about 35 ppmv. In the atmosphere, it is spatially variable and short-lived, having a role in the formation of ground-level ozone. The recommendation of the World Health Organization (1999) is that the exposure times should not exceed those shown in Table 3.

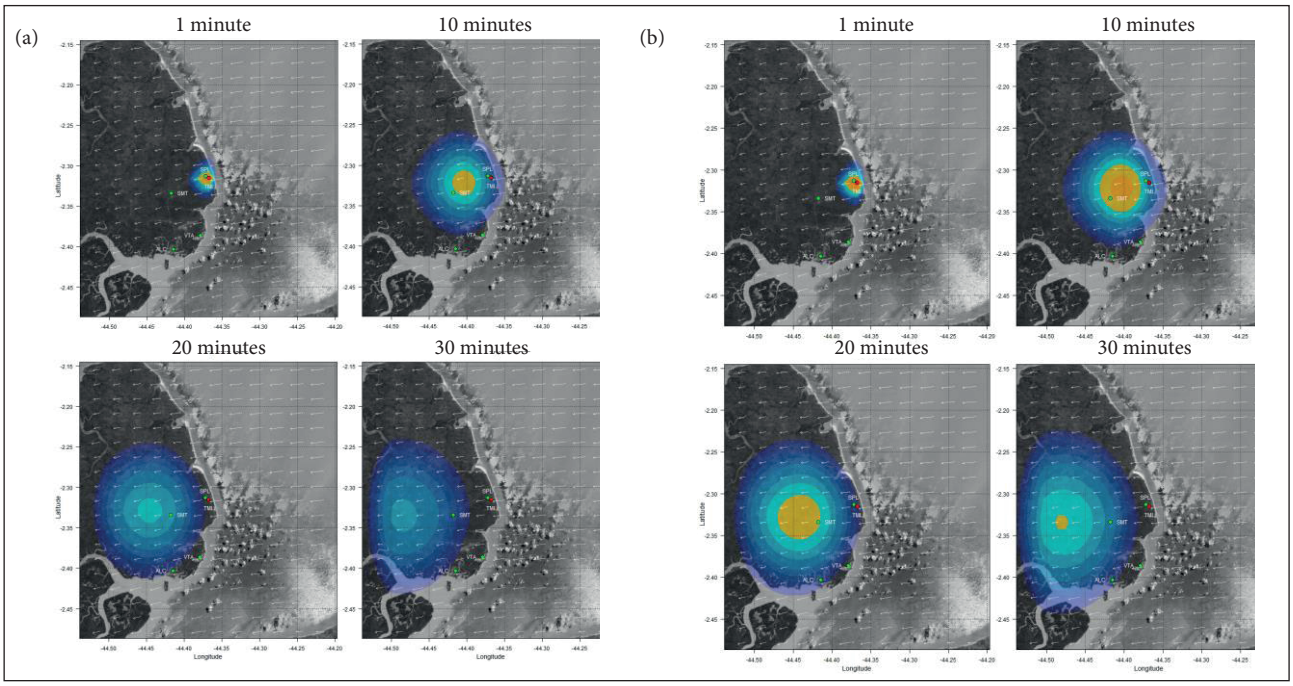

Figure 4. Surface concentrations after launching of (a) HCl and (b) CO.

Table 3. Exposure limits for CO.

CO exposure limits (ppmv)	Maximum exposition time
9	8 h
26	1 h
52	30 min
87	15 min
1,950	Rapidly fatal

Source: extracted from Winter and Miller (1976).

Figure 5a shows a time series of the HCl concentrations (presented in a logarithm scale) for up to 2 h after the launching for the locations SPL, SMT, CLA, and VTA. The higher levels are between 1,540 ppmv (SPL) and 176 ppmv (SMT) and, according to Table 2, the maximum exposure time is only 1 h; the inhalation of the gas can cause swelling of the lungs, throat spasm, and irritation. In the surrounding area, it presents concentration levels between 0.11 ppmv (VTA) and 0.53 ppmv (CLA), which are safety values of HCl, with effects imperceptible to the majority of the population.

Figure 5b presents the CO concentrations in function of time. The higher levels are in the range between 2,735 ppmv at SPL and 176 ppmv at SMT. From Table 2, a maximum exposure time is between 30 min and 2 h, and this may cause headache, increased heart rate, dizziness, nausea, and even death. In the surrounding area, it presents concentration levels below 2 ppmv (CLA and VTA), which are safety for the mankind.

Figure 5c shows the concentration of the CO_2 with a peak of 598 ppmv at SPL. It is considered the minimal value for an effect on health by CO_2 inhalation of 15,000 ppmv during 1 month of exposure. In practical sense these values of CO_2 concentration have no effect for the humans.

Figure 6 shows the particulate material with 10- and 2.5-mm concentrations composed by Al_2O_3 in function of time. The levels for the CLA and the VTA are below 1 mg/m^3.

The World Health Organization (2000) guidelines do not recommend the use of levels of pm 10 and pm 2.5 as long as there are no sufficient data to enable the derivation of specific values at present. Nevertheless, the large body of information on studies relating day-to-day variations in particulate matter to day-to-day variations in health provides quantitative estimates of the effects of particulate matter that are generally consistent. The available information does not allow a judgment to be made on concentrations below, in which no effects would be expected.

On the other hand, the Conselho Nacional do Meio Ambiente (Brasil 1990) presents some critical levels for monitoring purposes of the air quality in Brazilian territory for pm 10 and pm 2.5: attention case for 250 mg/m^3, alert for

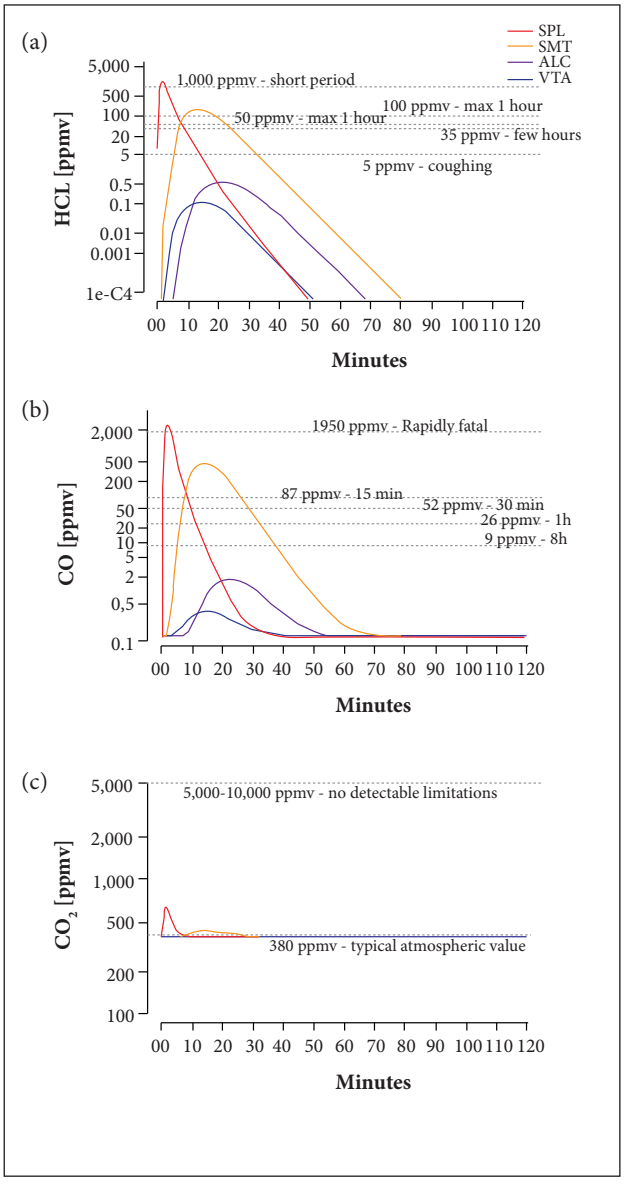

Figure 5. Time series of simulated and the levels of health effects for (a) HCl; (b) CO and (c) CO_2.

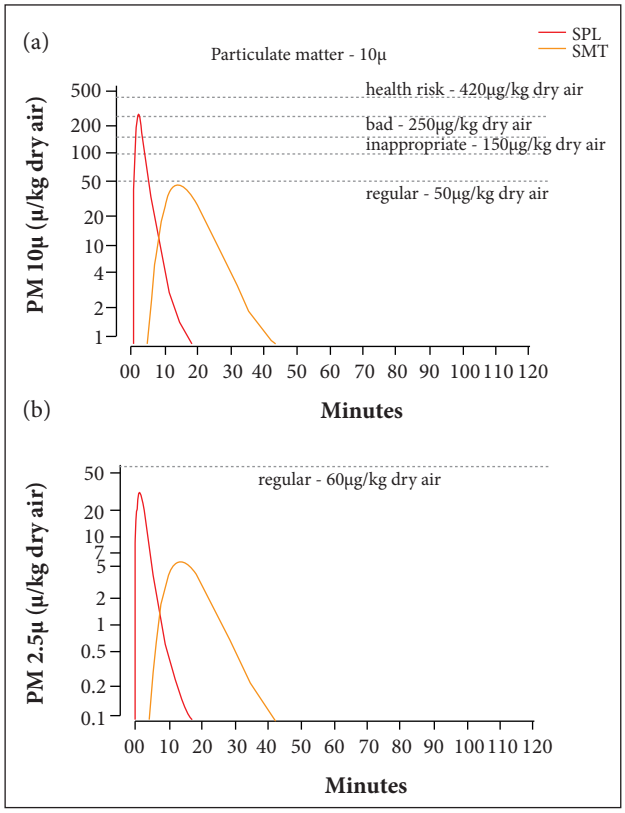

Figure 6. Time series of simulated and the levels of health effects for (a) pm 10 and (b) pm 2.5.

420 mg/m^3, and emergency for values beyond 500 mg/m^3. These values are for both pm 10 and pm 2.5, being calculated as an average during a time interval over 24 h. The maximum values for the pm 10 and pm 2.5 are 30.3 and 273.5 mg/m^3, respectively. The peak concentration of pm 10 is below the regular level adopted (50 mg/m^3), considered a secondary air quality standard or, in other words, a level in which it provides the minimum adverse effect on human health. However, the pm 2.5 concentration peaks are next to the attention level, but the mean value for the first hour is approximately 14 mg/m^3.

CONCLUSION REMARKS

In this paper we present a way to include the major atmospheric pollutants emissions from the VLS into a weather model (WRF-Chem) taking into account the vertical distribution of emission and the effect of buoyancy of the hot cloud formed by the effluents. This implementation represents an improvement to the study of Iriart and Fisch (2016), in which the emissions were made only at the surface level (without accounting the effect of buoyancy, trajectory, and variable emissions rates), not considering HCl; this features allowed us to use data from the Brazilian rocket VLS (instead of Titan-IV data) and analyze more realistic concentrations at the closer sites of the VLS launcher pad as the plume behavior for the CLA region.

The results show that the HCl levels are dangerous in the first hour after the launching at the SPL and SMT regions; the CO levels are more critical for the first 10 min after the launching, representing a high risk at the proximities of the SPL and attention state on the SMT. The concentrations of CO_2, pm 2.5, and pm 10 showed secure levels even for the proximities

of the SPL; finally, the exhaust cloud does not reached the CLA or the VTA, mainly due to the wind direction.

After 40 min of the VLS launching the clouds were dispersed and left the inner domain, which is the region of interest. This means that the levels of each pollutant are below the minimum concentration for a detectable effect on the human health.

As the transport and dispersion of the rocket effluents depend tightly on the atmosphere state, the simulations are not a general solution for the problem, but represent a very good prediction scenario. Stronger or weaker winds (or different wind directions) can make the transport more or less efficient (as well as allow the plume to reach different locations), and different stability conditions (stable or unstable) will affect the dispersion by reducing the turbulent mixing, resulting in higher (or lower) concentrations. Other simulations for different atmospheric stability and wind directions will be made for more general assumptions and case studies.

In a future study, we will focus our attention on the chemical mechanism, where the afterburn and HCl atmospheric reactions must be included into the chemical module of WRF for a more realistic representation of the atmospheric chemical influence of the effluents of rocket exhausts.

ACKNOWLEDGEMENTS

The authors thank the Coordenação de Aperfeiçoamento de Pessoal de Nível Superior (CAPES), who funded part of this research through the project PRO-ESTRATEGIA (number 2240/2012), as well as provided the scholarship grant PQ (number 308011/2014). At last, but not least, a special thanks to Dr. Stacy Walters, from The University Corporation for Atmospheric Research (UCAR), who contributed for this study with a very important support.

AUTHOR'S CONTRIBUTIONS

Schuch D performed the experiments and prepared the figures. Schuch D and Fisch G discussed the results and commented on the manuscript.

REFERENCES

Bjorklund JR, Dumbauld JK, Cheney CS, Geary HV (1982) User's manual for the REEDM (Rocket Exhaust Effluent Diffusion Model) computer program. NASA Contractor Report 3646. Huntsville: NASA George C. Marshall Space Flight Center.

Brasil. Ministério do Meio Ambiente (1990) Resolução CONAMA nº 3, de 28 de junho de 1990; [accessed 2017 Jan 19]. http://www.mma.gov.br/port/conama/legiabre.cfm?codlegi=100

Braxter PJ, Adams PH, Cockcroft A, Harrington JM (2000) Hunter's diseases of occupations. 9th ed. London: Arnold; New York: Oxford University Press.

Briggs GA (1975) Plume rise predictions. Lectures on Air Pollution and Environmental Impact Analysis. Amer Meteor Soc (72-73):59-111. doi: 10.1007/978-1-935704-23-2_3

Cencetti M, Veilleur V, Albergel A, Olry C (2011) SARRIM: A tool to follow the rocket releases used by the CNES Environment and Safety Division on the European Spaceport of Kourou (French Guyana). Int J Environ Pollut 44(1-4):87-95. doi: 10.1504/IJEP.2011.038406

Damian V, Sandu A, Damian M, Potra F, Carmichael GR (2002) The kinetic preprocessor KPP – a software environment for solving chemical kinetics. Comput Chem Eng 26(11):1567-1579. doi: 10.1016/S0098-1354(02)00128-X

Denison MR, Lamb JJ, Bjorndahl WD, Wong EY, Lohn PD (1994) Solid rocket exhaust in the stratosphere: plume diffusion and chemical reactions. J Spacecraft Rockets 31(3):435-442. doi: 10.2514/3.26457

Emmons LK, Walters S, Hess PG, Lamarque JF, Pfister GG, Fillmore D, Granier C, Guenther A, Kinnison D, Laepple T, Orlando J, Tie X, Tyndall G, Wiedinmyer C, Baughcum SL, Kloster S (2010) Description and evaluation of the Model for Ozone and Related chemical Tracers, version 4 (MOZART-4). Geosci Model Dev 3:43-67. doi: 10.5194/gmd-3-43-2010

Grell GA, Peckham SE, Schmitz R, McKeen SA, Frost G, Skamarock WC, Eder B (2005) Fully coupled "online" chemistry within the WRF model. Atmos Environ 39(37):6957-6975. doi: 10.1016/j.atmosenv.2005.04.027

Iriart PG, Fisch G (2016) Uso do modelo WRF-Chem para a simulação da dispersão de gases no Centro de Lançamento de Alcântara. Rev Bras Meteorol 31(4):610-625. doi: 10.1590/0102-7786312314b20150105

Lide DR (2003) CRC handbook of chemistry and physics. 84th ed. Boca Raton: CRC Press.

Moreira DM, Trindade LB, Fisch G, Moraes MR, Dorado RM, Guedes RL (2011) A multilayer model to simulate rocket exhaust clouds. J Aerosp Technol Manag 3(1):41-52. doi: 10.5028/jatm.2011.03010311

Nascimento EGS, Moreira DM, Fisch G, Albuquerque TTA (2014) Simulation of rocket exhaust clouds at the Centro de Lançamento de Alcântara using the WRF-CMAQ modeling system. J Aerosp Technol Manag 6(2):119-128. doi: 10.5028/jatm.v6i2.277

Nyman RL (2009) NASA Report: Evaluation of Taurus II Static Test Firing and Normal Launch Rocket Plume Emissions.

Pfister GG, Parrish DD, Worden H, Emmons EK, Edwards DP, Wiedinmyer C, Diskin GS, Huey G, Oltmans SJ, Thouret V, Weinheimer A, Wisthaler A (2011) Characterizing summertime chemical boundary conditions for airmasses entering the US West Coast. Atmos Chem Phys 11:1769-1790. doi: 10.5194/acp-11-1769-2011

R Core Team (2015) R: A language and environment for statistical computing; [accessed 2016 Apr 28]. https://www.R-project.org/

Rajasekhar M, Kumar MD, Subbananthan T, Srivastava V, Apparao B, Rao VS, Prasad M (2011) Exhaust dispersion analysis from large solid propellant rocket motor firing using HYSPLIT model over Satish Dhawan Space Centre (SDSC SHAR). Proceedings of the Indo-US Conference-cum-Workshop on "Air Quality and Climate Research"; Hyderabad, India.

Skamarock WC, Klemp JB, Dudhia J, Gill DO, Baker DM, Duda MG, Huang XY, Wang W, Powers JG (2008) A description of the Advanced Research WRF version 3. Technical Note. Boulder: National Center for Atmospheric Research.

Stockwell WR, Kirchner F, Kuhn M, Seefeld S (1997) A new mechanism for regional atmospheric chemistry modeling. J Geophys Res 102(D22):25847-25879. doi: 10.1029/97JD00849

Winter PM, Miller JN (1976) Carbon monoxide poisoning. J Am Med Assoc 236(13):1502-1504. doi: 10.1001/jama.1976.03270140054029

World Health Organization (2000) Air quality guidelines for Europe. WHO regional publications: European series, n. 91; [accessed 2016 Apr 20]. http://www.euro.who.int/__data/assets/pdf_file/0005/74732/E71922.pdf

World Health Organization (1999) Environmental Health Criteria 213: carbon monoxide. 2nd ed.; [accessed 2015 Oct 28]. http://www.who.int/ipcs/publications/ehc/ehc_213/en/

Yarwood G, Rao S, Yocke M, Whitten G (2005) Updates to the carbon bond chemical mechanism: CB05. Final report to the U.S. EPA, RT-0400675; [accessed 2016 May 19]. http://www.camx.com/files/cb05_final_report_120805.aspx